Kinematics Under Extreme Waves

Carl Trygve Stansberg
MARINTEK,
P.O. Box 4125 Valentinlyst,
N-7450 Trondheim, Norway
e-mail: carltrygve.stansberg@marintek.sintef.no

Ove T. Gudmestad
e-mail: otg@statoil.com

Sverre K. Haver
e-mail: svha@statoil.com

Statoil,
N-4035 Stavanger, Norway

Nonlinear contributions in near-surface particle velocities under extreme crests in random seas can be important in the prediction of wave loads. Four different prediction methods are compared in this paper. The purpose is to observe and evaluate differences in predicted particle velocities under high and extreme crests, and how well they agree with measurements. The study includes linear prediction, a second-order random wave model, Wheeler's method [1970, "Method for Calculating Forces Produced by Irregular Waves," JPT, J. Pet. Technol., pp. 359–367] and a new method proposed by Grue et al. [2003, "Kinematics of Extreme Waves in Deep Water," Appl. Ocean Res., **25***, pp. 355–366]. Comparison to laboratory data is also made. The whole wave-zone range from below still water level up to the free surface is considered. Large nonlinear contributions are identified in the near-surface velocities. The results are interpreted to be correlated with the local steepness kA. Some scatter between the different methods is observed in the results. The comparison to experiments shows that among the methods included, the second-order random wave model works best in the whole range under a steep crest in deep or almost deep water, and is therefore recommended. The method of Grue et al. works reasonably well for $z>0$, i.e., above the calm water level, while it overpredicts the velocities for $z<0$. Wheeler's method, when used with a measured or a second-order input elevation record, predicts velocities fairly well at the free surface $z=\eta_{max}$, but it underpredicts around $z=0$ and further below. The relative magnitude of this latter error is slightly smaller than the local steepness kA_0 and can be quite significant in extreme waves. If Wheeler's method is used with a linear input, the same error occurs in the whole range, i.e., also at the free surface.* [DOI: 10.1115/1.2904585]

Keywords: marine technology, hydrodynamics, ocean waves, kinematics

1 Introduction

Estimating the loads on offshore structures in extreme irregular waves is sensitive to the wave kinematics model used. In particular, contributions from nonlinear effects in wave-zone particle kinematics up to the free surface in random seas can be important, and have therefore been addressed throughout several studies in recent years. Traditionally, in addition to linear modeling, Wheeler's method [1] has been frequently used in engineering applications. In a review study on different methods, Gudmestad [2] found that Wheeler's method underpredicts the velocities under steep irregular waves, and he identified a need for further research. Another method is the second-order random wave modeling described in Stansberg [3], Stansberg and Gudmestad [4], using the formulation by Marthinsen and Winterstein [5]. This method has not yet been very widely in use for kinematics descriptions, (while, on the other hand, the related problem of extreme crest elevation is now quite frequently being modeled by second-order methods, see, e.g., Ref. [6]). Recently, a new method has been suggested by Grue et al. [7]. These three methods, plus the linear model, are compared in the present study. In addition, a part of the work also includes comparisons to selected experimental velocity data from the NHL-LDV (laser Doppler velocimetry) study by Skjelbreia et al. [8].

Due to their simplicity, and reasonable agreement in moderate sea states, the Wheeler method and the linear model are still in frequent use today for engineering applications also in extreme sea states. However, based on the above mentioned and other recent experiences, there is a need to address this practice. A general feeling of uncertainties related to the correctness of using the traditional Wheeler method for calculating kinematics under extreme waves, combined with the interesting report of Grue et al. [7], have been the main reasons for revisiting the present subject.

Three different sources of data are considered:

(a) purely numerical second-order simulation data, including regular, bichromatic, and irregular waves
(b) measured irregular elevation records from MARINTEK Ocean Basin laboratory data
(c) measured irregular elevation records from NHL-LDV data, also including measured velocities

Within the scope of the present study, some selected large and steep wave events in the time domain are considered, while a more systematic analysis based on complete irregular records is planned for future studies.

2 Linear Reference Model and Normalization

We shall use the commonly used linear wave model as a reference. A thorough description is given in several textbooks, see, e.g., Dean and Dalrymple [9], and we do not go into details of that description here. In the wave zone, linear orbital wave velocities are modeled up to the calm water surface and are assumed to be constant around this level. In the following, $u^{(1)}(z,t)$ shall denote the linear velocity time series at a vertical level $z\leqslant 0$, while $u_0(t)\equiv u^{(1)}(0,t)$ shall denote the linear horizontal velocity amplitude at $z=0$.

In this paper, data will be normalized with respect to the linear velocity amplitude u_0. For each selected event in the time domain, the velocity parameters will be transformed in the following way, for both regular, bichromatic as well as for irregular wave records: All velocities are divided by the corresponding linear velocity $u_0(t)$ at $z=0$. For purely numerical simulations, $u_0(t)$ is directly found from the linear input wave elevation record $\eta_0(t)$ by use of the linear velocity transfer function, written in the frequency domain as

Contributed by the Ocean Offshore and Arctic Engineering Division of ASME for publication in the Journal of Offshore Mechanics and Arctic Engineering. Manuscript received November 7, 2006; final manuscript received August 22, 2007; published online June 9, 2008. Assoc. Editor: Carlos Guedes Soares.

$$U(\omega) = \omega A(\omega) \frac{\cosh k(h+z)}{\sinh kh} \quad (1)$$

where $U(\omega)$ is the modulus of the Fourier transform of the linear orbital velocity $u_0(t)$ at $z=0$, $A(\omega)$ is the Fourier transform modulus of the corresponding wave elevation $\eta_0(t)$, ω is the angular wave frequency, k is the angular wave number, and h is the water depth. ω is related to k through the linear dispersion relation:

$$\omega^2 = gk \tanh kh \quad (2)$$

For numerical reconstructions of measured elevation records, u_0 is found, in the same manner, from a linear wave elevation component $\eta_0(t)$ estimated from the measured record. For each crest event in the time domain, the vertical level z is normalized by multiplication with the linear angular wave number k_0 locally estimated for the actual wave crest, found from the linear wave component in the following way:

$$k_0 \equiv \frac{\omega_0^2}{g} \quad (3)$$

(Hence, k_0 is actually the linear deep-water wave number corresponding to ω_0). The local angular wave frequency ω_0 is defined from the linear wave elevation and velocity time series $\eta_0(t)$, $u_0(t)$ at the crest peak, by using the approximation of regular-wave theory:

$$\omega_0 \equiv \frac{u_0}{A_0} \frac{\sinh kh}{\cosh k(h+z)} \quad (4)$$

where g is the acceleration of gravity, and A_0 is the linear crest height of the actual random event.

3 Nonlinear Correction Methods

Three different nonlinear methods for the prediction of wave-zone particle velocities $\mathbf{u}$ up to the free surface are compared and benchmarked to the linear model:

(a) second-order model
(b) method of Grue et al.
(c) Wheeler's method

In this comparison, we focus on the horizontal velocity u_x under the peaks $A \equiv \eta_{\max}$ of selected wave crests. In particular, extreme (steep) waves in irregular-wave trains on deep or almost deep water are considered. A few examples on regular and bichromatic waves are also addressed. Unidirectional waves are assumed. We consider this assumption to be conservative with respect to the extreme velocities, in accordance with the findings by Johannessen et al. [10].

Second-Order Model. Time series of horizontal velocities are consistently modeled at any vertical level up to the linear free-surface wave elevation $A_0(t) \equiv \eta_{\text{linear}}(t)$ by use of the second-order irregular-wave modeling in Refs. [3,4], which was based on the formulation in Ref. [5]. A linear input wave record is used, which can be either purely numerical or extracted from measurements. Arbitrary water depth can be modeled in the present version. Full storm durations, typically 3 h, can be modeled.

The horizontal velocity amplitude at a level z under a crest is formulated as

$$u^{\text{tot}}(z) = u^{(1)}(z) + u^{(2,\text{sum})}(z) + u^{(2,\text{diff})}(z), \quad z \leqslant 0$$

$$u^{\text{tot}}(z) = u_0 + \left.\frac{\partial u^{(1)}}{\partial z}\right|_{z=0} z + u^{(2,\text{sum})}(0) + u^{(2,\text{diff})}(0), \quad z > 0 \quad (5)$$

where $u^{(2,\text{sum})}$ and $u^{(2,\text{diff})}$ are the contributions from the sum- and difference-frequency potentials, respectively. For more details, we refer to the above references. Roughly speaking, in deep water, this model represents a linear extrapolation of the linear velocity gradient for $z>0$, plus a second-order difference-frequency potential term, which is generally negative under energetic wave groups.

Note that in deep water the sum-frequency velocity potential is zero, and for regular waves also the difference-frequency contribution is zero then. In finite waters, this is modified, but in almost deep water the modifications are small. An essential item in the model is the choice of the low-pass filter in the tail of the linear spectrum, which is needed in order to assure consistency in the perturbation to second order. Here, we use the cutoff criterion proposed in Stansberg [11] for deep-water waves: $\omega_{\text{high}} \equiv \sqrt{(k_{\text{high}} g)}$, where $k_{\text{high}}=2/H_s$. Comparisons to experimental data have indicated that this reasonably works well [4]. A discussion of this criterion was also made by Brodtkorb [12].

Method of Grue *et al.* A new method has been proposed in Grue et al. [6], based on observations from fully nonlinear wave simulations and from experimental results in a wave flume. Steep deep-water transient waves and similar events are considered. The method is phenomenological but has some physical basis in third-order Stoke's regular-wave theory. It is intended for use on individual waves one by one, from observed crest heights and wave periods only. It is rather simple and is therefore potentially an interesting method.

The hypothesis is that the vertical profile of the horizontal velocity is simply given by

$$u_x(z) = u_0' \exp(k'z) \quad (6)$$

with the normalized reference velocity at $z=0$ defined as

$$u_0' = \varepsilon' \sqrt{\frac{g}{k'}} \quad (7)$$

Here k' is the actual (nonlinear) angular wave number $2\pi/L$, L is the wave length, and ε' is a steepness parameter. In Ref. [7], ε' is implicitly found from measurements, see Eqs. (8) and (9) below. (Invoking third-order Stokes theory, we identify it as $k'A_0$, where A_0 is the linear crest height, while neither A_0 nor $k'A_0$ are explicitly expressed in the original reference). If linear theory is valid, Eq. (7) reduces to $u_0'=\omega' A_0$.

The nonlinear wave number k' and the steepness ε' used in this formulation are given by the following third-order Stokes regular-wave formulation

$$k' \eta_{\max} = \varepsilon' + \frac{1}{2}\varepsilon'^2 + \frac{1}{2}\varepsilon'^3 \quad (8)$$

$$\frac{\omega'^2}{gk'} = 1 + \varepsilon'^2 \quad (9)$$

Following the procedure in Ref. [7], we find the wave frequency ω' from the trough-to-trough period T_{TT} observed from the wave time series. This differs from the definition chosen for the other methods, Eq. (4). For narrow-banded spectra, the two definitions do not differ significantly. For broad-banded spectra, there may be some deviations. In the identification of troughs, we use a zero-crossing criterion, unless otherwise stated. In the original, referred procedure, also the crest height $\eta_{\max}$ is found from the measurement.

The method is based on a regular-wave theory; thus, in its basic form, it does not take into account any low-frequency difference-frequency contributions (i.e., the return flow). There are, however, ways to take the return flow into account in this procedure, although we have not made use of such here.

Comments on Definitions and Notations. The estimated wave frequency ω' and wave number k', defined in the method of Grue et al. above, are generally different from those used elsewhere in this study. In order to distinguish the parameters from the others, we have therefore identified the present ones by use of the asterisk *. The differences partly arise because the local wave period definitions differ. Furthermore, the wave number k' is nonlinear and decreases with increasing steepness, while a linear wave number definition is used in the other methods. In this study, we also find it convenient to define a "linear" wave number k'_0 found directly from T_{TT}:

$$k'_0 \equiv \frac{\omega'^2}{g}, \quad k' = \frac{k'_0}{1+\varepsilon'^2} \tag{10}$$

This linear wave number is generally different from the one defined for the other methods (k_0), due to another wave period definition as mentioned above.

Also, the present reference velocity u'_0 is differently defined from a corresponding parameter used in the other methods. The normalizing velocity unit is given in Eq. (7): $u'_0=\varepsilon' \sqrt{(g/k')}$, which can be written in terms of the parameters ω_0, ω', u_0, A_0, and k' above:

$$u' = u_0 \frac{\dfrac{\omega'}{\omega_0}}{\sqrt{[1+(k'A_0)^2]}} \tag{11}$$

(to third order). This means that the present normalized velocity at $z=0$ in general differs from 1, and in most cases it will be somewhat lower. As a result, graphs from use of the method of Grue et al. will in general appear shrinked (or sometimes stretched) on our plots relative to what they would have looked like using their definitions directly.

Wheeler's Method. The method proposed by Wheeler [1] is widely in use since it is simple and it takes into account an observed reduction from linear predictions around $z=0$. At the same time, when a measured record is used as input, it also predicts reasonable free-surface velocities. The basic principle is that from a given elevation record, one computes the velocity for each frequency component using linear theory, assuming each component to be freely propagating (although they are in reality nonlinear in the higher frequency tail of the spectrum). Then, for each time step in the time series, the vertical (z) coordinate is "stretched" from the original level z to a level z':

$$z' = \frac{z-\eta}{1+\dfrac{\eta}{d}} \tag{12}$$

where η is the elevation and d is the water depth. Thus, for deep water, it simply implies a time-varying vertical shift following the elevation.

It should be noted that if a linear input elevation record is used, the method transforms (stretches) the linear fluid velocities up and down according to the elevation. Thus, there may be a significant velocity reduction under high crests relative to the linear model throughout the whole water column in the wave zone. The relative magnitude of this reduction is approximately equal to the normalized vertical shift $k_0\eta_{\max}$:

$$\frac{\Delta u}{u_0} = \exp(k_0\eta_{\max}) - 1 \approx k_0\eta_{\max} \quad \text{(in deep water)} \tag{13}$$

If, on the other hand, a nonlinear (e.g., a measured or a second-order) elevation record is used as input, nonlinear components will add as if they were independent and "free" near the free surface. It can be shown analytically that for a *deep-water regular wave*, a purely second-order elevation input will give exactly the same free-surface velocity as the consistent second-order model.

The consistent second-order model gives, from Eq. (5),

$$u^{\text{tot}}(z=A_0) = u_0 + \left(\frac{\partial_u}{\partial_z}\bigg|_{z=0}\right) z = u_0 + \omega k_0 (A_0)^2 \tag{14}$$

while Wheeler's method with a second-order elevation input gives

$$u^{\text{free surface}} = u_0 + 2\omega A^{(2)} = u_0 + 2\omega[0.5k_0(A_0)^2] = u_0 + \omega k_0(A_0)^2 \tag{15}$$

where we have used the fact that the second-order elevation component is $A^{(2)}=0.5k_0(A_0)^2$ (from Stokes theory). The above effect is strongly reduced or vanished around $z=0$ and below, in which region the Wheeler method will predict the same velocities as with a linear input.

When using a measured input record, a low-pass filter is needed in order to avoid too high frequencies leading to excessive free-surface velocity estimates. A reasonable filter choice procedure can be trying to include linear plus second-order contributions only, since that will lead to a free-surface velocity reasonably close to that of the consistent second-order model (see the paragraph above). In practice, $f_{\text{cut}} \approx 4 f_{\text{peak}}$, where f_{cut} is the cutoff frequency and f_{peak} is the spectral peak frequency, often leads to a useful result.

4 Data Sets

Numerical Simulations. Linear and second-order numerical deep-water wave simulations are made by use of MARINTEK's in-house software for modeling of second-order wave kinematics, based on the formulations given in Refs. [3–5,11]. Four different cases are run, see Table 1. One particular crest event is considered for each of the cases. A JONSWAP spectrum formulation with gamma=2.5 was used for the spectrum. Deep water is assumed.

The maximum local steepnesses kA shown in the table are defined from actual crest event parameters in the time domain as described previously in Sec. 2.

Ocean Basin Elevation Measurements. A measured elevation record from an earlier experiment with extreme waves in MARINTEK's Ocean Basin is used as input to wave-zone kinematics estimation. Only elevation was measured, not kinematics

The wave spectrum data are given in Table 1 (full scale). A 10,000 year Norwegian Sea storm sea state, with a two-peaked Torsethaugen spectrum formulation, is used. One particular time-domain event with a large and steep wave is selected from the time series here. The model scale was 1:55, and the water depth was 335 m, i.e., deep water. Waves were measured without any structure in the basin.

From the measurements, the linear (free) wave component is extracted using a second-order filtering technique followed by the low-pass filtering procedure described previously for the second-order model.

Wave Flume Data Including Kinematics Measurements. Selected measurements from an earlier LDV experiment [8], made in a wave flume at NHL, Trondheim, are considered. The wave spectrum data are described in Table 1. A JONSWAP spectrum formulation is used. Results are here scaled up 80:1 from the original data so that the sea state corresponds approximately to an

Table 1 Summary of data sets used in study (wave heights *H* in meters; periods *T* in seconds *kA*=maximum "linear" local wave steepness in selected events)

	Regular			Bichromatic					Irregular		
	H	T	kA	H_1	H_2	T_1	T_2	kA	Hs	Tp	kA
Numerical simulations	7.6 21.6	12.0 12.0	0.1 0.3	11.9	5.6	15.0	9.0	0.40	16.0	14.0	0.38
Ocean basin experiment									20.0	20.0	0.38
NHL-LDV experiment									17.6	16.0	0.35 0.39

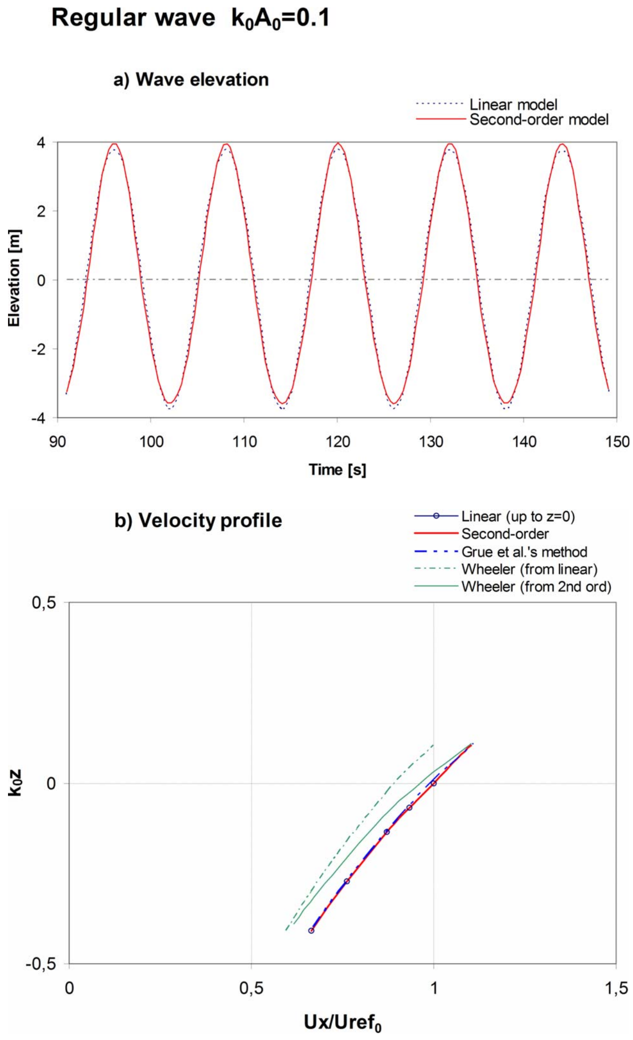

Fig. 1 (*a*) Elevation time series and (*b*) normalized horizontal velocity profile under crest peak. Regular wave numerical simulation. Moderate steepness $k_0A_0=0.10$.

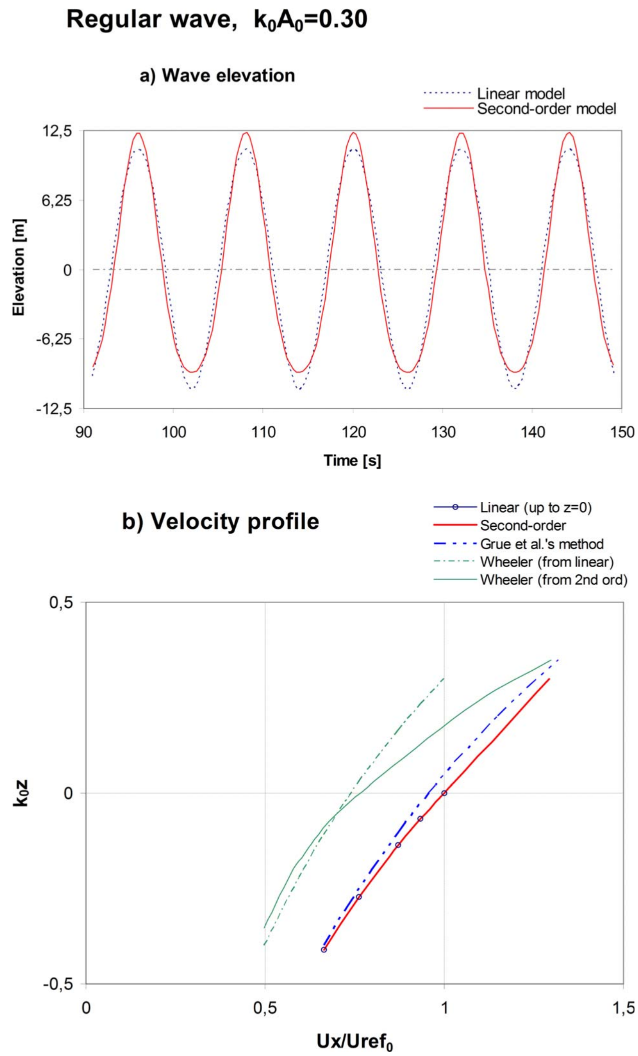

Fig. 2 As Fig. 1, but high steepness $k_0A_0=0.30$

extreme storm condition. The water depth corresponds to 104.5 m, i.e., deep water for wave periods $T<11.5$ s. Two different events are selected among the largest in a run with approximately 500 waves. Waves were measured without any structure in the basin.

In addition to surface elevations, particle velocities were measured at fixed vertical (z) level with 4 m intervals in the wave zone. The experiment was repeated for each z level.

5 Examples From Results

Regular and Bichromatic Waves. Elevation time series samples and corresponding, normalized velocity profiles under crests are shown in Figs. 1–3. These cases include numerical simulations only. Details of the actual wave conditions are given in Table 1. The regular waves include one moderate and one high steepness case. (Notice that, according to the formulation defined in the previous chapters, the steepness parameter k_0A_0 refers to the linear or free wave component of the actual record and not to the total nonlinear wave.) The bichromatic wave is steep, especially around the extreme peak where the superposition of the two components leads to a local steepness corresponding to near breaking.

The elevation plots include linear and second-order modeling. Velocity profile models include the following:

(a) linear model (up to $z=0$)
(b) second-order model
(c) method of Grue et al.
(d) Wheeler's method, using linear input
(e) Wheeler's method, using second-order input

The regular-wave velocity profile plots clearly demonstrate that the second-order profile coincides with the linear one up to $z=0$, while above this, it simply follows the linear extrapolation k_0z. Grue et al.'s method follows quite well the second-order model. Wheeler's method shows too low velocities, especially below the free surface (use of second-order input compensates for this near the surface).

In the bichromatic case, the second-order model shows a reduction around $z=0$ and below, in accordance with the negative (return) current arising due to the setdown effect under energetic groups, even in deep water. This effect is less pronounced for the method of Grue et al. Wheeler's method shows significantly lower velocities at $z=0$ in this very steep case.

Irregular Waves. Elevation time series and velocity profile plots for selected extreme events in steep irregular waves are presented in Figs. 4–7. Details on the sea states are given in Table 1. Figure 4 shows a purely numerical wave, while the other three figures shows wave events from laboratory records, and the measured elevation is then also included in the time series plots. In two of the figures (Figs. 6 and 7), the velocity profiles also include

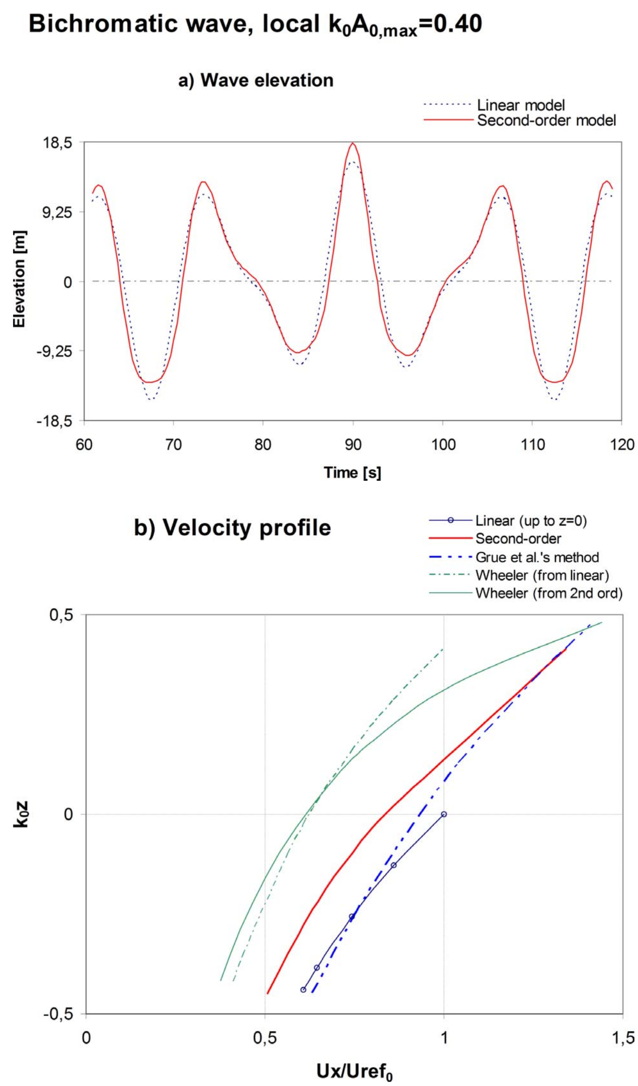

Fig. 3 (*a*) Elevation time series and (*b*) normalized horizontal velocity profile under extreme crest peak. Bichromatic wave numerical simulation. Local max steepness $k_0A_0=0.40$.

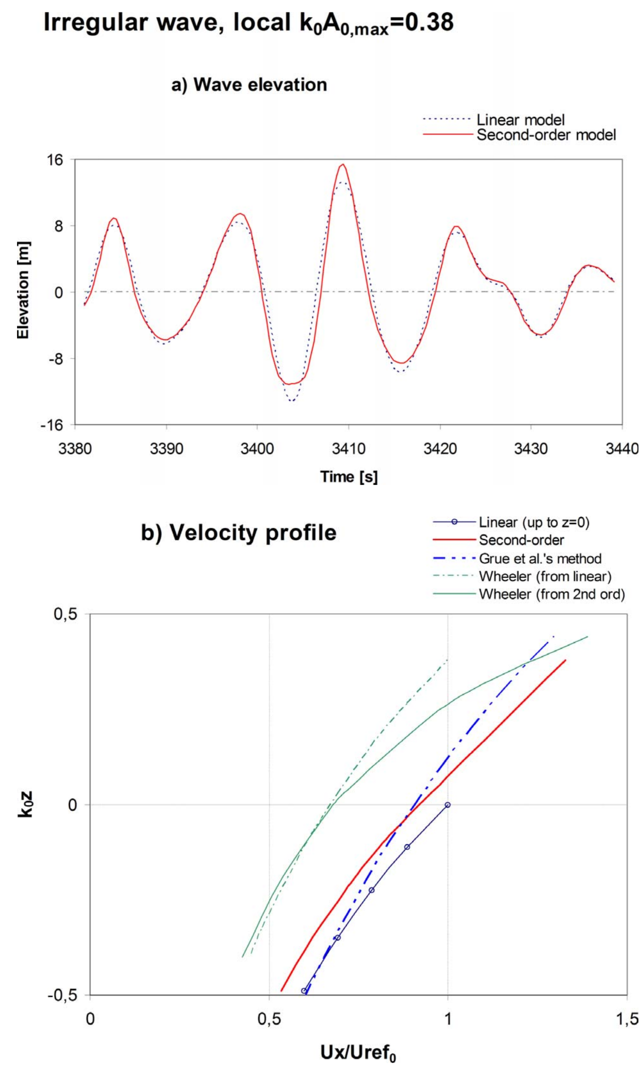

Fig. 4 As Fig. 3, but irregular-wave event from numerical simulation. Local max steepness $k_0A_0=0.38$.

measured velocities from the NHL-LDV measurements [8].

With measured elevation available, the Wheeler prediction with second-order elevation input (used in the purely numerical studies) is now replaced by measured input.

As far as the comparison of the different models is concerned, these plots demonstrate similar characteristics as those of the bichromatic case in Fig. 3. One should also notice that the local steepnesses are in the same high range, from 0.35 to 0.40, which is near the classical breaking criterion for regular waves (0.42).

The comparison to measurements shows that the second-order elevation reproduces reasonably well the measured nonlinear sharpening and enhancement of crest, and flattening of troughs. Still it is missing a portion of the extreme crest peak level, which is not surprising considering the high local steepness.

Measured velocity profiles compare reasonably well to those of the second-order and the model of Grue et al. in the water column above the mean water level. At $z=0$ and below, the second-order model seems to compare quite well.

6 Discussion

In the lower wave zone $z<0$, all nonlinear models generally predict lower velocities than the linear model for irregular waves. This is also confirmed by the measured velocity data. For $z>0$, linear data cannot be defined (and should be assumed to be constant—equal to u_0), while all the other models show increased velocities with increasing z, in agreement with the measurements. At the free surface, predicted velocities are up to 1.3–1.5 times u_0 in the steepest events. The "performances" of each of the different nonlinear models are discussed in the following.

The second-order model is the one that compares best with the LDV measurements of the selected test run, both with respect to the gradient for $z>0$ and with respect to the reduction (relative to linear) at $z<0$. The difference observed at the highest measurement level in Event 1 may be due partly to higher-order effects, but the possible measuring uncertainty at such measurement points with a very short fluid measurement duration should also be kept in mind. Furthermore, all examples (numerical and experimental) show that for $z>0$ the predicted gradient of the normalized velocity agrees reasonably well with k_0z or is slightly higher. This is a helpful result, indicating that the regular-wave approximation in the estimation of the local k_0 works quite well. The choice of the low-pass filter for the input spectra, based on a criterion taking into account the perturbation problem, seems to have been satisfactory. It is, however, recommended to address this further, e.g., through sensitivity studies. Another possible topic to study further is the consequencues from the use of such a nonlinear kinematic model on statistical properties of velocities and possible forces and responses.

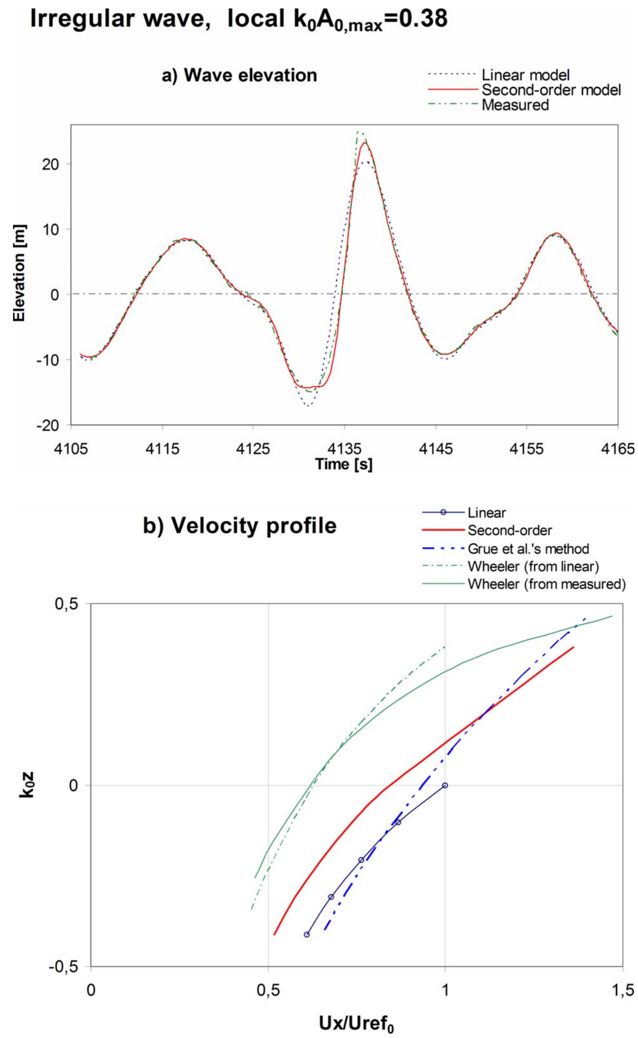

Fig. 5 (*a*) Elevation time series and (*b*) normalized horizontal velocity profile under extreme crest peak. Irregular-wave event, ocean basin experiment. Local max steepness $k_0A_0=0.38$.

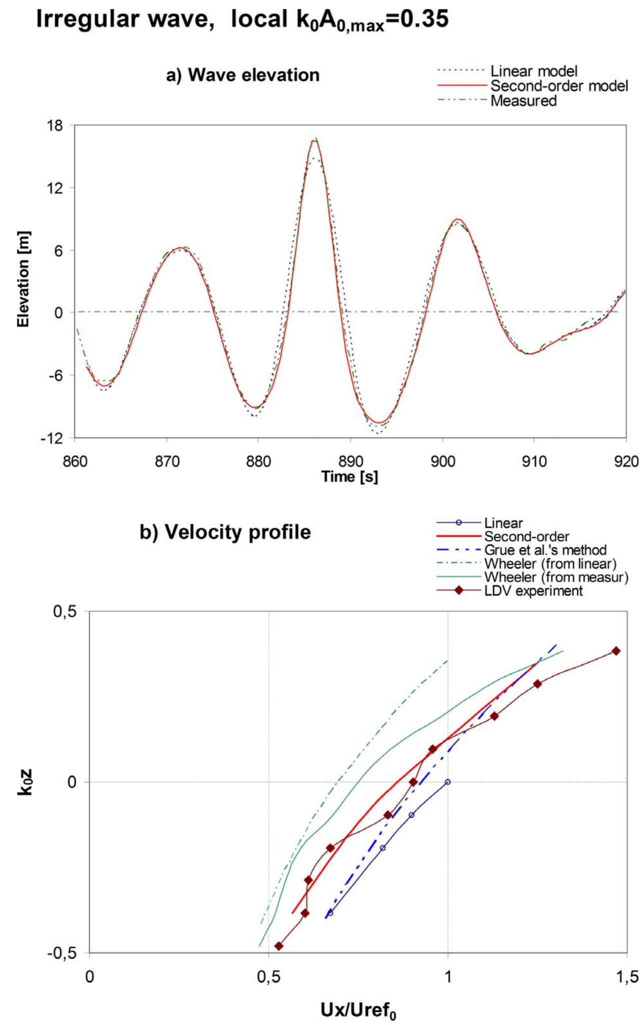

Fig. 6 (*a*) Elevation time series and (*b*) normalized horizontal velocity profile under extreme crest peak. Irregular-wave event, NHL-LDV experiment (Event 1). Local max steepness k_0A_0 =0.35.

The method of Grue et al. compares fairly well both with the measurements and with the second-order model in the zone $z>0$. It is, however, not always quite robust with respect to the trough-to-trough estimation of the wave period T', since for irregular waves there may sometimes be alternative and equally logical choices for this estimation, except for narrow-banded spectra. It is not clear from the definition in the original reference whether a zero crossing or a local minimum trough criterion is used in their work. In our work, we have basically used zero crossing, but our experience also indicates that a local minimum criterion may, in fact, work better. More systematic studies should be made to clarify this. Furthermore, the method basically neglects the negative return current effect for $z<0$ under energetic wave groups, although a minor effect is in most cases still apparently predicted near $z=0$ due to the higher-order wave length elongation reducing the reference velocity u_0'. Some overprediction at levels below $z=0$ can also be identified in the original results [7], which qualitatively confirms our finding.

Wheeler's method, if based upon a linear wave elevation record only, significantly underpredicts the velocities at all depth levels. The relative error is in the range of $0.5k_0A_0-0.75k_0A_0$, where k_0A_0 is the local steepness.

If Wheeler's method is based on a nonlinear record, e.g., upon a second order or a measured time series, the velocity predicted near the surface is clearly improved compared to the linear input case above. However, it rapidly decreases with z, and at $z=0$ and below the relative underprediction is typically $0.5k_0A_0-0.75k_0A_0$s as with a linear input record. The rapid decrease is strongest for the steepest waves—hence the method may be a fairly reasonable choice for low-steepness waves. For a typical individual design wave in the North Sea with $H=29$ m, $T=15$ s, k_0A_0 is approximately 0.26. Assuming a second-order input record then, use of Wheeler's method will predict reasonably well at the free surface, while it will be expected to underpredict by approximately 10–20% in the region around $z=0$ and below. Another item, which makes the method less robust, is the need to define a low-pass filter for a measured input wave signal, to avoid excessive high-frequency contributions. In a way, this problem may appear to be similar to the filtering problem in the second-order model, but the difference is that in the Wheeler method case, there seems to be no clear physical criterion behind the filter choice. One reasonable criterion, however, might be to try to filter away all contributions of order higher than 2, since use of a pure second-order model as input gives a free-surface velocity reasonably close to a consistent second-order model (but it still predicts too low velocities further down in the fluid).

In this paper, we have made limited selections from large data sets. In the underlying work, comparisons for more examples were made, which generally support the findings shown here. Still, there is a need to include a wider variety of data for a more

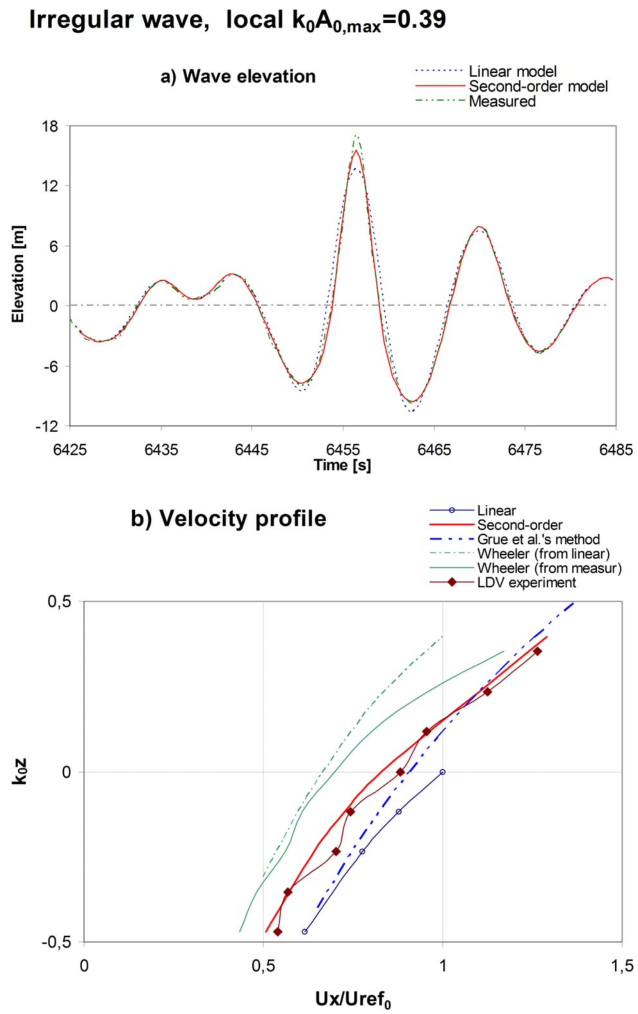

Fig. 7 As Fig. 6, but another event (Event 2). Local max steepness $k_0A_0=0.39$.

systematic study. A limitation has also been made in the selection of methods. Further work with a broader scope is therefore suggested.

7 Conclusions

At the free surface of steep crests, $z=\eta_{\max}$, all of the three nonlinear methods predict the maximum velocity reasonably well, except when Wheeler's method is used with linear input in which case a significant underprediction is observed. The maximum velocities are typically 30–40% higher than linear predictions. At lower levels in the wave zone, there are larger discrepancies between the models. An overall conclusion is that among the methods investigated here, the second-order random wave model works best at all levels of the water column under a steep crest in deep water, and is therefore recommended. The method of Grue et al. works reasonably well in most cases for $z>0$, i.e., above the calm water level, while it generally overpredicts the velocities for $z<0$. Wheeler's method, when used with a measured or a second-order input elevation record, predicts fairly well the velocities at the free surface, but it underpredicts around $z=0$ as well as at lower levels. The relative magnitude of this underprediction is slightly lower than the local steepness k_0A_0 and can be quite significant in extreme waves. If Wheeler's method is used with a linear input, the same error occurs also at the free surface.

Further work is recommended to compare the different methods in a more systematic way and also in a broader range of sea states, not only selected events in extreme conditions as focused on here. A broader study could also include a more comprehensive comparison to a larger set of related results in the literature. Furthermore, a sensitivity analysis of the low-pass filter needed in the second-order random wave model is needed to establish it as a robust model. Finally, the consequences from the present findings on the resulting wave loads, such as drag forces on slender structures and wave slamming loads, and their statistical properties, should be investigated.

Acknowledgment

This study has been financed by Statoil. The authors gratefully acknowledge the permission to publish this paper. Experimental kinematics data were obtained from the SINTEF NHL Wave Kinematics Experiment (1988–1991), which was financed by NTNF, Statoil, Amoco, Conoco, Exxon, and Mobil.

References

[1] Wheeler, J. D. E., 1970, "Method for Calculating Forces Produced by Irregular Waves," JPT, J. Pet. Technol., pp. 359–367.

[2] Gudmestad, O. T., 1993, "Measured and Predicted Deep Water Wave Kinematics in Regular and Irregular Seas," Mar. Struct., **6**, pp. 1–73.

[3] Stansberg, C. T., 1994, "Second-Order Effects in Random Wave Modeling," *Proceedings of International Symposium on Waves—Physical and Numerical Modeling*, Vancouver, Canada, Vol. 2, pp. 793–802.

[4] Stansberg, C. T., and Gudmestad, O. T., 1996, "Nonlinear Random Wave Kinematics Models Verified Against Measurements in Steep Waves," *The 15th OMAE Conference*, Florence, Italy, Vol. IA, pp. 15–24.

[5] Marthinsen, T., and Winterstein, S., 1992, "On the Skewness of Random Surface Waves," *Second ISOPE Conference*, San Francisco, CA, Vol. 3, pp. 472–478.

[6] Forristall, G., 1998, "Wave Crest Distributions: Observations and Second-Order Theory," *Conference on Ocean Wave Kinematics, Dynamics, and Loads on Structures*, ASCE, Houston, TX, pp. 372–382.

[7] Grue, J., Clamond, D., Huseby, M., and Jensen, A., 2003, "Kinematics of Extreme Waves in Deep Water," Appl. Ocean. Res., **25**, pp. 355–366.

[8] Skjelbreia, J. E., Berek, G., Bolen, Z. K., Gudmestad, O. T., Heideman, J. C., Ohmart, R. D., Spidsøe, N., and Tørum, A., 1991, "Wave Kinematics in Irregular Waves," *Proceedings of the Tenth OMAE Conference*, Stavanger, Norway, Vol. IA, pp. 223–228.

[9] Dean, R. G., and Dalrymple, R. A., 1991, *Water Wave Mechanics for Engineers and Scientists*, World Scientific, Singapore, Chap. 4.

[10] Johannessen, T. B., and Swan, C., 2001, "A Laboratory Study of the Focusing of Transient and Directionally Spread Surface Water Waves," Proc. R. Soc. London, Ser. A, **457**, pp. 971–1006.

[11] Stansberg, C. T., 1998, "Non-Gaussian Extremes in Numerically Generated Second-Order Random Waves on Deep Water," *The Eighth ISOPE Conference*, Montreal, Canada, Vol. III, pp. 103–110.

[12] Brodtkorb, P. A., 2004, "The Probability of Occurrence of Dangerous Wave Situations at Sea," Dr. ing. thesis, NTNU, Trondheim.